CrystEngComm

Cite this: *CrystEngComm*, 2012, **14**, 1582

www.rsc.org/crystengcomm

PAPER

Raman spectroscopic imaging of indomethacin loaded in porous silica

Sanna Hellstén,*[a] Haiyan Qu,[b] Teemu Heikkilä,[c] Jarno Kohonen,[a] Satu-Pia Reinikainen[a] and Marjatta Louhi-Kultanen[a]

Received 20th April 2011, Accepted 28th November 2011
DOI: 10.1039/c2ce05471j

Loading of a poorly soluble drug such as indomethacin (IMC) into porous silica particles enhances its dissolution upon administration. The distribution of the different solid forms in which IMC may appear was studied using Raman spectroscopy. Raman mapping of the samples was performed with a Raman microscope equipped with an automated *xy*-stage. The spectral data were extracted in the range 1500–1750 cm^{-1}, which represents the stretching of the C=O bond in the IMC molecule. To alleviate the problem of overlapping peaks in the Raman spectra of the different IMC forms, the spectral data were analyzed using partial least squares (PLS) and principal component analysis (PCA). Despite the problems caused by fluorescence, the method gave valuable information about the occurrence and distribution of the solid forms of IMC. The same approach was utilized for analysis of the heterogeneity of recrystallized IMC samples, and PCA was shown to be capable of revealing the presence of solvates or polymorphs not included in the model.

1 Introduction

Following the introduction of methods such as high-throughput screening and combinatorial chemistry in drug discovery in the mid-1990s, poor solubility has become an issue in oral drug delivery. One method developed for the enhancement of the bioavailability of a poorly soluble active pharmaceutical ingredient (API) is to load the API in a carrier material that is able to increase both its solubility and dissolution rate. The effect is based on the increased surface area of the API and confinement stabilization of the API inside the pores in a solid form with a higher solubility, typically the amorphous form. Ordered porous silica particles, *e.g.*, SBA-15 and MCM-41, can be used for such a purpose.[1,2]

The API is typically loaded into the silica particles using a solution immersion method.[3] The aim is to fill the pores evenly with a maximum amount of the API. The approach is not wholly unproblematic. Crystallization on the particle surface should be prevented, since it would result in hindered dissolution and reduced bioavailability upon administration. Crystallization may also occur inside the pores. A compound confined in a porous matrix may possess different polymorphism than in the bulk material.[4] Furthermore, the chemistry of the surface on which the crystallization occurs may result in selective crystallization of a certain polymorph.[5] As different crystal forms of the API may have distinct properties, such as bioavailability and stability, it is of major importance to carefully characterize the solid form of the drug loaded in the porous particles.

The presence of a crystalline surface fraction can be detected using differential scanning calorimetry (DSC) since the melting point reveals whether the crystalline drug is on the surface or inside the pores. The aim of this paper is to use a new method, Raman mapping and multivariate data analysis, to obtain more information about the distribution of the solid forms of an API possibly crystallized on the loaded silica particles. Indomethacin (IMC) is used as the model compound.

IMC has several polymorphs, α and γ being the most common.[6–8] These two polymorphs together with amorphous IMC can be expected to be present in IMC loaded silica particles. Determination of the crystallinity of IMC based on Raman spectroscopy has been demonstrated by Taylor and Zografi.[9]

More recently, Heinz *et al.*[10] have quantified ternary mixtures of the different forms of IMC using partial least squares (PLS). A similar approach is utilized in the present investigation of IMC loaded silica particles. In addition, principal component analysis (PCA) is applied for detection of any anomalous spectra which might be related to the presence of solvent residuals in the crystal structure. Such residuals could be expected, since IMC has a strong tendency towards solvate formation in many solvents, *e.g.*, in methanol.[8,11]

2 Materials and methods

Three different types of samples were prepared for Raman analyses. First, mixtures of the pure solid forms of IMC were

[a]*Lappeenranta University of Technology, Department of Chemical Technology, Skinnarilankatu 34, FI-53850 Lappeenranta, Finland. E-mail: sanna.hellsten@lut.fi; Fax: +358 5 621 2199; Tel: +358 40 448 9105*
[b]*University of Southern Denmark, Institute of Chemical Engineering, Biotechnology and Environmental Technology, Niels Bohrs Allé 1, DK-5230 Odense M, Denmark*
[c]*University of Turku, Department of Physics and Astronomy, Turku University, FI-20014, Finland*

prepared to form a calibration set. Second, ordered mesoporous silica particles were loaded with IMC. For these samples, the effect of stressing at high temperature and humidity on the physicochemical stability of the samples was also investigated. Third, IMC was recrystallized from hot ethanol, akin to the loading procedure of silicas, and from methanol, as it is a known IMC solvate former.[8,11]

IMC (commercial γ-form) purchased from Hawkins, Inc. was used as received. Amorphous IMC for calibration measurements was produced by heating γ-IMC in a DSC to 165 °C at 10 °C min^{-1} and then cooling it rapidly. α-IMC was prepared by the anti-solvent precipitation method of Kaneniwa *et al.*[12] Seven calibration samples consisting of α-, γ- and amorphous IMC in different portions based on the Simplex-centroid design were prepared by gently mixing the components in a mortar.

SBA-15[13,14] and MCM-41[15,16] silica particles were prepared using methods described elsewhere. The prepared mesoporous silica materials were gently ground in a ball mill and the resulting fine white powder was passed through mesh number 230 (63 μm) or 120 (125 μm) test sieves using a sieve shaker apparatus. The sieved particles were loaded with IMC using a solution immersion method. The loading was carried out in hot ethanol solution (68 °C) in order to raise the concentration of the poorly soluble drug in the solution to the level required for efficient loading of silica mesopores (250 mg ml^{-1}). The loaded samples were stored in a dry desiccator prior to analysis. In order to study the physicochemical stability of the loaded drug under stressed conditions, some of the samples were stored at 30 °C and 60% relative humidity for 3 months in a desiccator with a saturated sodium bromide salt solution. Amorphous IMC has been shown to transform into the crystalline form under these conditions.[17] The preparation, loading and stressing procedure of the silica particles are described in more detail in ref. 18. The morphology of the silica particles was characterized by imaging on a Cambridge S200 SEM and the particle size distributions of the samples were measured using a Malvern Mastersizer 2000 laser diffraction instrument equipped with a Hydro 2000G wet dispersion sampler. The porosity (surface area and pore volume/diameter) of the silica particles was characterized with nitrogen (N_2) adsorption/desorption measurements on a Micrometrics Tristar 3000 instrument at −196 °C. The results are presented in Table 1. Additional characterization of the silica particles before and after loading, as well as after stressing by several methods (XRD, DSC, TGA, ATR-FTIR, HPLC), can be found in ref. 18.

The recrystallized samples of free IMC were prepared from methanol (analytical grade, Merck) at 36 °C and from ethanol (Etax Aa, Altia) by drying the saturated solutions to constant weight. Drying was performed either at reduced pressure (700–800 mbar) at 36 °C or at ambient pressure at a temperature of 35 °C or 65 °C. IMC was also freely recrystallized from boiling ethanol (in an oven at 100 °C) in an attempt to produce a high fraction of chemically degraded drug in the sample, in order to evaluate its effect on Raman analysis. The complete removal of solvent from the samples recrystallized from methanol was verified by thermogravimetric (TG) analysis using a Netzsch STA 449 C with helium purge and a heating rate of 10 °C min^{-1}. The recrystallized free IMC samples were stored in a dry desiccator prior to analysis.

Table 1 Morphological characteristics of mesoporous silica MCM-41 and SBA-15 particles. D_v50, D_{BJH}, S_{BET} and V_p refer to 50% particle undersize volume by laser diffraction and BJH pore diameter, BET surface area and BJH total pore volume by N_2 adsorption/desorption, respectively

	Particle shape	D_v50/μm	D_{BJH}/nm	S_{BET}/m^2 g^{-1}	V_p/cm^3 g^{-1}
SBA/125	Acicular	26.9	8.3	597	0.880
SBA/63	Modular	22.4	7.9	535	0.709
MCM/125	Granular	78.0	2.5	935	0.789
MCM/63	Modular	36.1	2.5	909	0.785

2.1 Raman spectroscopy

Raman spectroscopy measurements were done using a Horiba Jobin-Yvon LabRam 300 Raman microscope equipped with a CCD detector and an external cavity stabilized single mode diode laser at 785 nm. The spectrometer was daily calibrated at 0 and 520.7 cm^{-1} with a standard silicon sample. The laser power delivered to the sample was around 100 mW. No specific sample pretreatment was required; the samples were only gently pressed between two glass plates to obtain a smooth surface.

Calibration samples and the recrystallized IMC samples were analyzed with a confocal aperture of 400 μm, slit width of 150 μm, and exposure time of 20 s with two accumulations. 48 spectra were collected for each sample. The spectra were used individually in the data treatment and the final results were averaged.

In the Raman mapping of the IMC loaded silica particles the confocal hole was set to 1000 μm and the slit width to 100 μm. Spectra were captured using an acquisition time of 15 s with two accumulations. Spectra were collected throughout the sample surface utilizing an automated *xy*-stage. The aim was to cover an area of 2.4 × 2.4 mm with a spot size of 100 μm.

Since the particle size (Table 1) of SBA-15 and MCM-41 was smaller in comparison to the spot size of the Raman microscope, the distribution of IMC in a single particle could not be determined with the method used. Instead, the aim of the analysis was to screen the surface of an adequate amount of the sample powder. The averaged information obtained is more relevant considering the application of the drug loaded particles in pharmaceutical formulations such as tablets, where a relatively large amount of particles is contained in a single dose.

2.2 Data analysis

The spectral data were extracted in the range 1500–1750 cm^{-1}, which represents the stretching of the C=O bond in the IMC molecule.[19] Baseline correction was performed using a line segment method in LabSpec software. This pre-treatment reduced the baseline effects of fluorescence that occurred especially with samples containing amorphous IMC. MATLAB was used for further data treatment.

The spectral data collected from the calibration samples were divided into a calibration dataset and a test set, both representing one-half of the spectra for each sample. The spectral data, matrix $\boldsymbol{X}$, were mean centered. For the response matrix $\boldsymbol{Y}$, which consisted of the known fractions of the three components in the

samples, autoscaling was performed, *i.e.*, the data were centered and each variable was divided by the corresponding standard deviation. The PLS model was evaluated based on the degree of explained variance (R^2) of matrix $\boldsymbol{Y}$.

The PCA model was created using the same calibration series as for the PLS model. Multivariate control charts were utilized for detection of outliers and identification of solvate spectra.

3 Results and discussion

Raman spectra of the solid forms of IMC present in the IMC loaded silica particles are shown in Fig. 1. A characteristic peak for α-IMC occurs at a wavenumber of 1650 cm^{-1}. The spectrum of amorphous IMC has a broad band at around 1681 cm^{-1}, and the γ-polymorph shows a sharp peak at 1699 cm^{-1}. As seen in the figure, the peaks partially overlap, which hinders interpretation of the spectra using univariant methods commonly applied to Raman spectra. The relative intensities at certain wavenumbers do, however, give insight into the composition of the samples when compared with reference samples representing the pure solid forms.

To enhance the reliability of the results, multivariate modeling was applied. Four PLS latent variables (LVs) were included in the calibration model based on cross-validation. The percentages of the spectral variation explained by each LV are presented in Table 2. The low R^2 value for $\boldsymbol{Y}$ (46.38%) is reasonable because the response value of a spectrum collected from a calibration sample was the average composition of the sample. The true, local composition related to a particular spectrum, which actually represents a very small part of the sample only, may differ from the average composition if the sample is not completely homogeneous. The IMC calibration samples were likely to be somewhat inhomogeneous because only a gentle mixing was performed in order to avoid phase transformations. A plot comparing the observed and calculated fractions of three solid forms is presented in Fig. 2. Variation can be observed in the case of mixture samples.

In the PCA model, four principal components were included. The total variance captured was 98.14%.

3.1 Composition of the samples

The determined fractions of the different solid forms of IMC in the loaded silica particles are presented in Table 3. The results represent the average of *n* spectra. The measurement depth of the Raman microscope is dependent on the sample material, and in the case of the mesoporous silica material loaded and covered with IMC, it was not possible to estimate the exact penetration depth of the measurement. Hence, the values presented in Table 3 can be used for comparison between the samples only. The results represent the average of the compositions determined for all the spectra collected from the sample in question. The spectra of the sample SBA/125/IMC and the corresponding stressed sample SBA/125/IMC/S are presented in Fig. 3. As seen in the figure, there are characteristics of both amorphous and crystalline IMC in the spectra.

As can be seen in Table 3, the number of measurements varies; burning of the sample prevented spectra being collected through the whole sample. Furthermore, the stressed MCM-41 samples and the smaller size fraction of SBA-15 could not be analyzed at all, since they were so vulnerable to burning. The tendency towards burning was clearly related to the color of the sample. The stressed samples of IMC loaded silica had turned brownish or reddish brown, as can be seen in Fig. 4, and thus absorbed the red laser more intensively. The poor thermal conductivity of porous silica strengthened the heating effect. In addition to the burning problem, severe fluorescence occurred with dark colored samples. The original color of the loaded silica particles was pale yellow, which obviously indicated the presence of yellow

Table 2 Percent variance captured by the four latent variables (LV) of the PLS model

	X-Block		Y-Block	
LV#	This LV	Total	This LV	Total
1	54.73	54.73	14.80	14.80
2	35.10	89.84	16.55	31.35
3	6.49	96.33	13.22	44.56
4	1.63	97.96	1.82	46.38

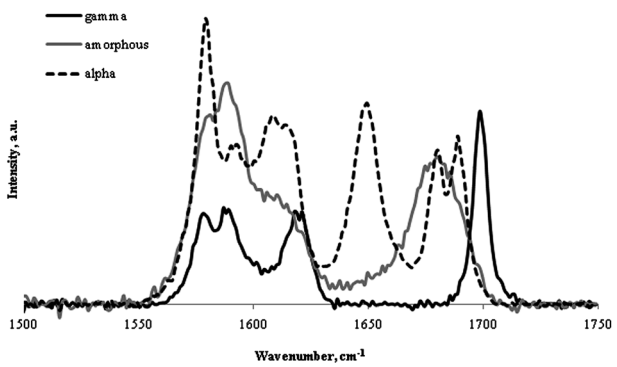

Fig. 1 Raman spectra of α- and γ-polymorphs and amorphous IMC.

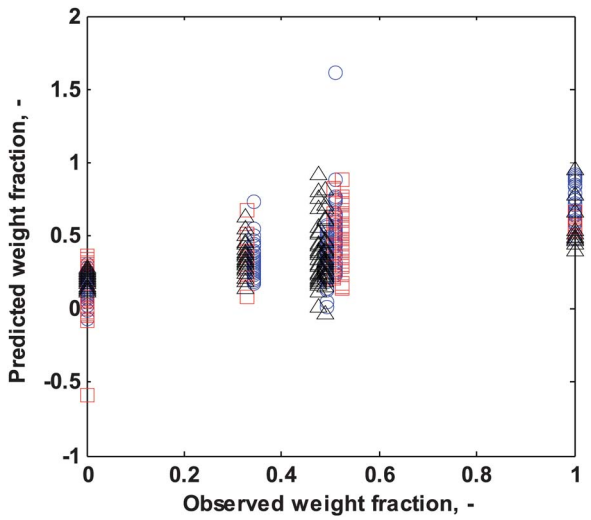

Fig. 2 The composition of the samples *versus* the composition predicted by the PLS model: α-IMC (blue circles), γ-IMC (red squares) and amorphous indomethacin (black triangles).

Table 3 Fractions of different IMC forms in loaded SBA-15 and MCM-41 particles of different sizes. Notation S refers to a stressed sample, and *n* is the number of spectra used in calculation

	α	γ	Amorphous	*n*
SBA/125/IMC	0.2937	0.3247	0.3816	576
SBA/125/IMC/S	0.2331	0.3364	0.4305	528
SBA/63/IMC	0.3293	0.3418	0.3289	336
MCM/125/IMC	0.2633	0.3028	0.4339	383
MCM/63/IMC	0.2578	0.2982	0.4440	143

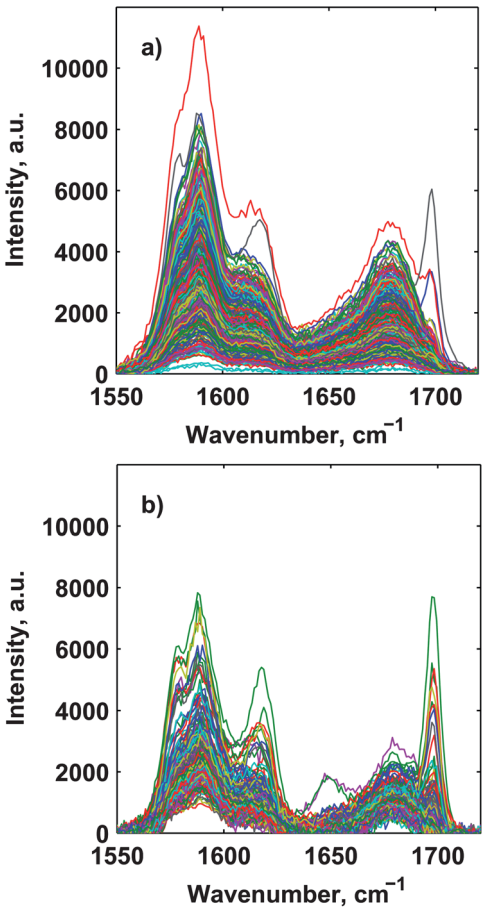

Fig. 3 The Raman spectra collected from samples SBA/125/IMC (a) and SBA/125/IMC/S (b).

amorphous IMC. The color change is probably related to degradation of IMC, especially upon stressing. HPLC purity analysis was performed on the samples, and a clear increase in the area of HPLC peaks at RRTs of 0.7 and 1.8, possibly related to IMC degradation products, was noted for the stressed samples. This was especially evident in the stressed MCM/125 and MCM/63 samples, in which also the color change was the most clear.[18] Degraded drug has been also previously linked to increased fluorescence in Raman analysis of indomethacin.[20,21]

Based on sample SBA/125, stressing results in a decrease in the overall crystallinity of the sample. This phenomenon might be related to the high humidity. The fraction of metastable α-IMC is lower in the stressed sample. It may have either transformed into stable γ-IMC or decomposed.

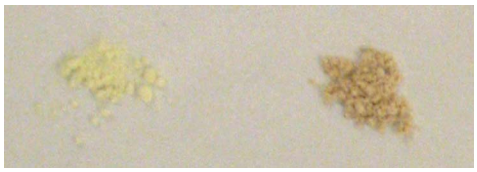

Fig. 4 Change in the color of sample MCM/63 upon stressing at high temperature and humidity. The non-stressed sample is on the left-hand side and the stressed sample on the right-hand side.

The results for the recrystallized free IMC samples are presented in Table 4. The samples recrystallized from ethanol consist mainly of the polymorph α, which is characteristic of IMC crystallized from ethanol.[8,6] As the temperature is increased from 35 °C to 65 °C, the fraction of this metastable form increases because of faster evaporation of the solvent. However, the sample recrystallized from boiling ethanol, in order to produce degraded IMC, seems to have lower α-IMC content. The result is most probably due to increased fluorescence caused by the degradation of IMC at high temperature, which was evident from the changed, brownish shade of color of the free IMC, akin to the loaded silica sample in Fig. 4. Fluorescence may also explain the apparent occurrence of the amorphous form in these crystalline samples. Reduction in the drying pressure did not have any notable effect on the results.

In IMC recrystallized from methanol, the results suggest that the sample consists mainly of the amorphous form. However, examination of the spectral data revealed that the spectra are not typical for amorphous IMC but rather for IMC methanolate, the spectrum of which is presented by Joshi.[22] The existence of a form that was not included in the calibration model is clearly confirmed by the squared prediction error of the residuals chart (SPE_X) in the PCA based multivariate statistical process control (MSPC).[23] On the other hand, some γ-IMC was also detected. Since no observable mass loss occurred in the TG analysis, it was suspected that the spectrum actually represents polymorph δ, which is known to be formed upon desolvation of IMC methanolate.[22] The presence of δ-IMC was actually confirmed by the differential thermal analysis (DTA) results simultaneously provided by the analyzer.

The PLS model could also be extended to include the solvate spectra. The production of representative samples for calibration is, however, a difficult task, since the majority of IMC solvates are non-stoichiometric. This means that the solvent is not bonded into the crystal structure to form a defined arrangement; it is just occluded in a random way. Quantification of the solvates

Table 4 Composition of recrystallized IMC samples based on *n* Raman spectra interpreted using PLS

	α	γ	Amorphous	*n*
At ambient pressure				
IMC/ethanol/35 °C	0.6840	0.1193	0.1967	96
IMC/ethanol/65 °C	0.7867	0.0331	0.1803	96
IMC/ethanol/100 °C	0.4952	0.2703	0.2345	96
At reduced pressure				
IMC/methanol/36 °C	0.2768	0.3018	0.4215	71
IMC/ethanol/36 °C	0.6735	0.0777	0.2487	68

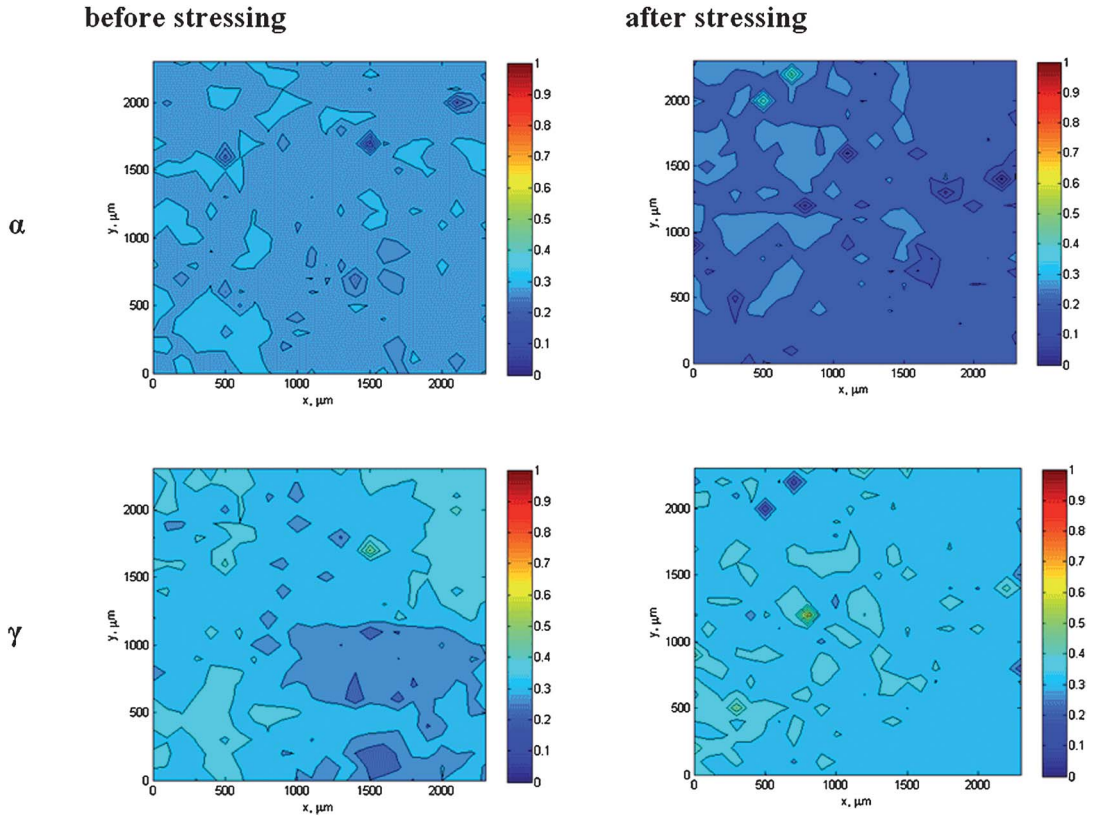

Fig. 5 Distribution of crystalline α- and γ-IMC in sample SBA/125/IMC before and after stressing at increased temperature and relative humidity according to PLS analysis. Color scales represent crystallinity (0 = fully amorphous, …, 1 = fully crystalline). Some more crystalline clusters or points were detected on the sample as a result of stressing, although overall the stressing seemed to result in a decrease of bulk crystallinity of the powder.

might not be relevant for the loaded silica particles, nor indeed other drug delivery systems, since the presence of occluded solvents would be totally unacceptable. Thus, the three-variable model combined with multivariate control charts was considered adequate in the case of IMC.

3.2 Distribution of the polymorphs

The distribution of the two polymorphs of IMC in one of the IMC loaded silica samples and the effect of stressing it at high temperature and humidity are illustrated in Fig. 5. The contour plots are interpolated from the results of PLS analysis at each measurement point of the Raman mapping.

Overall, the crystalline IMC was relatively evenly distributed on the particles. Thus, the homogeneity of the sample in terms of drug distribution was found to be good. A few separate clusters of IMC of higher crystallinity were detected, and the number of these clusters increased after stressing. In Fig. 5, two α-IMC crystals can be seen in the upper left part of the figure of the stressed sample and one γ-IMC crystal near the center of the figure. In contrast, no such crystalline clusters can be readily detected in the figures of the non-stressed sample. Thus, Raman imaging suggests that larger crystalline clusters are formed upon storage at higher temperature and humidity.

Considering the overall uniformity of the IMC recrystallized from ethanol, the samples prepared at higher temperatures showed more variance in their composition. This result is reasonable, since fast evaporation of solvent typically leads to less uniform crystallization.

3.3 Possible sources of error

The most significant source of error in the study was the mixing of the calibration samples. The samples were mixed gently in order to avoid mechanically induced solid phase transformations. The composition of the calibration samples was difficult to verify. For example, DSC was found to be an unfeasible method for validation, since re-crystallization occurred during analysis.

Other error sources may arise from the Raman measurements. Due to the novelty of Raman analysis of drug-loaded mesoporous silica particles, the possible effects of the carrier material in the spectra are not known. However, the pure silica materials did not give any significant Raman signal at the measurement conditions used. Some interaction between IMC and the silica surface may, however, exist and affect the spectra. Moreover, possible impurities and degradation products of IMC are not taken into account in the model. Another interfering factor in the measurement data may be the small day-to-day variance observed in the laser intensity.

4 Conclusions

The solid form of a compound determines many important pharmaceutical properties. It is of special importance to ensure

the occurrence of the right form of the API in a medicinal product because it is critical for both the stability and the therapeutic effects. Raman spectroscopy is a fast and convenient method for solid form studies. In this paper, Raman spectroscopic imaging combined with multivariate modeling was successfully utilized for characterization of drug-loaded mesoporous silica particles.

The results revealed the occurrence of two polymorphs and the amorphous form of a model compound, IMC, in the samples. In most cases, crystalline IMC seemed to be evenly distributed on the surface of the sample. Nevertheless, the results suggested formation of larger crystalline clusters upon storage of the samples at higher temperature and humidity. Such crystallization may affect the *in vitro*/*in vivo* drug release performance of porous silica–IMC formulations.

The analysis was influenced by the two major problems often encountered in Raman spectroscopy: fluorescence and sample burning. These problems could probably be prevented or alleviated by adjusting the measurement parameters and applying special pre-treatment techniques for the spectral data. Nevertheless, the results of this study showed that the possible degradation or color changes of the studied compound pose challenges in the development of the whole analysis method.

In the present study, the developed imaging method was also tested for recrystallized IMC samples. In some of these samples, pseudo-polymorphs, *i.e.*, solvates, of IMC were detected. Even a minor amount of these forms may change the Raman spectrum significantly. Therefore, the PLS based model, which was originally developed for investigation of three forms of IMC only, was shown to fail in determining the composition of the samples in which other forms were also present. However, Raman spectroscopy provided useful information of the presence of unexpected solid forms such as solvates or rare polymorphs. Based on PCA and MSPC, the SPE_X control chart was found to be a valuable tool in the detection of anomalous spectra.

In conclusion, Raman spectroscopic imaging combined with multivariate modeling provides information on the occurrence and distribution of the solid forms on the surface of porous silica particles. If combined with different analysis techniques such as DSC, the new method can bring better understanding of the crystallization behavior of the drug loaded in a porous carrier material.

Acknowledgements

Financial support from the Graduate School in Chemical Engineering and the Academy of Finland (project nos. 122314, 123037 and 122828) is acknowledged. Dr N. Kumar and Prof. D. Yu. Murzin from Åbo Akademi University are acknowledged for providing the silica particles.

References

1 M. Vallet-Regi, A. Rámila, R. P. del Real and J. Pérez-Pariente, *Chem. Mater.*, 2001, **13**, 308.
2 J. M. Rosenholm and M. Lindén, *J. Controlled Release*, 2008, **128**, 157.
3 C. Charnay, S. Bégu, C. Tourné-Péteilh, L. Nicole, D. A. Lerner and J. M. Devoisselle, *Eur. J. Pharm. Biopharm.*, 2004, **57**, 533.
4 J.-M. Ha, B. D. Hamilton, M. A. Hillmyer and M. D. Ward, *Cryst. Growth Des.*, 2009, **9**, 4766.
5 J. R. Cox, L. A. Ferris and V. R. Thalladi, *Angew. Chem., Int. Ed.*, 2007, **46**, 4333.
6 H. Yamamoto, *Chem. Pharm. Bull.*, 1968, **16**, 17.
7 L. Borka, *Acta Pharm. Suec.*, 1974, **11**, 295.
8 P. A. Slavin, D. B. Sheen, E. E. A. Shepherd, J. N. Sherwood, N. Feeder, R. Docherty and S. Milojevic, *J. Cryst. Growth*, 2002, **237–239**, 300.
9 L. S. Taylor and G. Zografi, *Pharm. Res.*, 1998, **15**, 755.
10 A. Heinz, M. Savolainen, T. Rades and C. J. Strachan, *Eur. J. Pharm. Sci.*, 2007, **32**, 182.
11 K. J. Crowley and G. Zografi, *J. Pharm. Sci.*, 2002, **91**, 429.
12 N. Kaneniwa, M. Otsuka and T. Hayashi, *Chem. Pharm. Bull.*, 1985, **33**, 3447.
13 D. Y. Zhao, Q. S. Huo, J. L. Feng, B. F. Chmelka and G. D. Stucky, *J. Am. Chem. Soc.*, 1988, **120**, 6024.
14 W. A. Hua, Y. H. Yue and Z. Goa, *J. Mol. Catal. A: Chem.*, 2001, **170**, 195.
15 C. T. Kresge, M. E. Leonowicz, W. J. Roth, J. C. Vartuli and J. S. Beck, *Nature*, 1992, **359**, 710.
16 A. Bernas, P. Laukkanen, N. Kumar, P. Mäki-Arvela, J. Väyrynen, E. Laine, B. Holmbom, T. Salmi and D. Y. Murzin, *J. Catal.*, 2002, **210**, 354.
17 H. Imaizumi, N. Nambuand and T. Nagai, *Chem. Pharm. Bull.*, 1980, **28**, 2565.
18 T. Limnell, T. Heikkilä, H. A. Santos and S. Sistonen, *et al.*, *Int. J. Pharm.*, 2011, **416**, 242.
19 A. Hédoux, Y. Quinet, F. Capet, L. Paccou and M. Descamps, *Phys. Rev. B: Condens. Matter Mater. Phys.*, 2008, **77**, 094205.
20 M. Savolainen, A. Heinz, C. Strachan and N. Sandler, *et al.*, *CRS Abstract*, 2007.
21 A. Heinz, M. Savolainen, T. Rades and C. J. Strachan, *Eur. J. Pharm. Biopharm.*, 2007, **32**, 182.
22 V. Joshi, PhD dissertation, Purdue University, 1999.
23 T. Kourti and J. F. MacGregor, *Chemom. Intell. Lab. Syst.*, 1995, **28**, 3.